E14-2008-200

M. Balasoiu[1,2], A. I. Kuklin[2], O. L. Orelovich[2],
Yu. S. Kovalev[2], G. M. Arzumanian[2],
T. S. Kurkin[3], S. V. Stolyar[4], R. S. Iskhakov[4], Yu. L. Raikher[5]

STRUCTURAL INVESTIGATIONS
OF BIOGENIC IRON OXIDE SAMPLES.
PRELIMINARY RESULTS

[1]National Institute of Physics and Nuclear Engineering, Bucharest, Romania
[2]Joint Institute for Nuclear Research, Dubna
[3]Institute of Synthetic Polymer Materials RAS, Moscow, Russia
[4]Siberian Federal University, Krasnoyarsk, Russia
[5]Institute of Continuum Media Mechanics, Ural Branch of RAS, Perm, Russia

Балашою М. и др.   E14-2008-200

Структурные исследования образцов биогенных окислов железа.
Предварительные результаты

    Представлены предварительные результаты исследования влияния продолжи-
тельности культивирования бактерии *Klebsiella oxytoca* на морфологию и струк-
туру биогенных частиц оксида железа. Результаты получены методами оптиче-
ской микроскопии, растровой электронной микроскопии и малоуглового рассе-
яния рентгеновских лучей.

    Работа выполнена в Лаборатории нейтронной физики им. И. М. Франка
ОИЯИ.

Balasoiu M. et al.   E14-2008-200

Structural Investigations of Biogenic Iron Oxide Samples.
Preliminary Results

    Some preliminary results on morphology and structure of iron oxide particles
formed inside *Klebsiella oxytoca* bacteria are presented. In particular, by means of
optical microscopy, scanning electron microscopy and small-angle X-ray scattering
the effect of the bacteria age (the duration of growth) on the nanoparticles properties
is studied.

    The investigation has been performed at the Frank Laboratory of Neutron Physics,
JINR.

INTRODUCTION

Intense research interest to nanoparticles is motivated by their unique physical properties, which are intermediate between the molecular level and the properties of the corresponding bulk materials. Studies of nanoparticles are important both from fundamental and technological points of view [1–3]. The particular scientific interest to magnetic nanoparticles is due to wide prospects of their technological applications in high density magnetic recording media, permanent magnets, magnetic refrigeration, magnetic sensing, etc. Biogenic iron oxides particles [4–6] make a separate class of magnetic nanoparticles that is of special interest for biomedical applications.

Of at least sixteen iron oxides distinguished in chemistry [7], ferrihydrite is one of the most important due to its rather wide spread in organic and mineral matter. It can be synthesized by rapid hydrolysis of Fe(III) solution, and its chemical formula is generally presented as $Fe_5HO_8 \cdot 4H_2O$, also written as $5Fe_2O_3 \cdot 9H_2O$ or as $Fe_2O_3 \cdot 2FeOOH \cdot 2.6H_2O$ [7–9]. Ferrihydrite is often present in soil and water systems [10] and is an essential ingredient in many industrial applications, metallurgy, in particular [11, 12]. It is encountered in many living organisms, bacteria, plants, fish and animals as well as in humans [13]. There it dwells in the form of ferritin: a mineral-protein complex that mainly serves for storage of iron that is excessive at the moment but might be needed and used immediately when iron gets in deficiency. There is some evidence also to the effect that ferritin plays an important role in maintaining a correct immunological assay of living organisms [14–16].

The precise structure of ferrihydrite is still a subject of debate. Two types of material are commonly called ferrihydrite: 2-line ferrihydrite (sometimes misleadingly termed protoferrihydrite) and 6-line ferrihydrite. These notations refer to the number of lines in their respective X-ray diffraction patterns. The 6-line ferrihydrite was identified as a mineral by International Mineralogical Association (IMA) since 1973 [17, 18]. The less crystalline 2-line ferrihydrite, on the other hand, is not believed to be a mineral. In comparison with most minerals, both 2-line and 6-line ferrihydrites show very broad diffraction lines that makes it difficult to extract accurate structural information. Notably, ferrihydrite only exists as a nanomaterial, yielding 2–4 nanometer crystals when in the 2-line form and 5–6 nanometer crystals when in the 6-line form [19–21].

With its high specific surface area [7], ferrihydrite is a very reactive substance. It can interact, either by surface adsorption or by co-precipitation, with a number of environmentally important chemical species, including arsenic, heavy metals, e. g., lead or mercury, with phosphates and many organic molecules. Thermodynamically, ferrihydrite is a metastable form of iron oxide and is known to be a precursor for more crystalline minerals like hematite and goethite [22].

In the present paper we investigate the samples containing biogenic iron nanoparticles (presumably, ferrihydrite) produced by bacteria *Klebsiella oxytoca.*

1. SAMPLE PREPARATION

The pelobiont microorganisms, which produce ferrihydrite nanoparticles, were discovered in sapropel of Lake Borovoe (Krasnoyarsk Region, Russia). The sample preparation method is described in detail in [5, 6]. Schematically, the bacteria are extracted with the aid of a magnetic separator and are inoculated onto an agarized medium where they are cultured under anaerobic conditions to obtain colonies. The matured biomass is further kept under microaerophilic conditions on an appropriate medium. There the ferric citrate concentration is varied from 0.2 to 5 g/l, the yeast extract concentration is maintained at 0.05 g/l, the benzoic acid is varied between 0.2 and 0.5 g/l. Samples are collected during the interval from 5 to 90 days after the micro-organisms are inoculated onto the nutrient medium. Figure 1 shows a micrograph of a bacterium on the 15th day of cultivating [5].
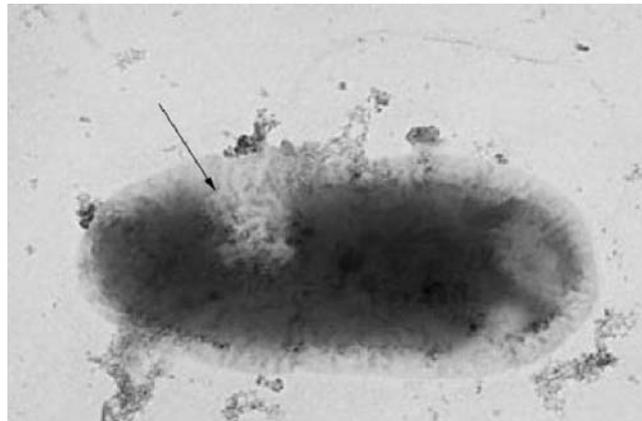
Fig. 1. The micrograph of the bacterium on the 15th day of cultivating [5]

The performed XRD-analyses indicate that the obtained particles are polycrystalline, have a cubic structure with lattice parameter $a = 8.39$ Å. The observed interplanar spacing of biomineral Fe-containing substances suggests the presence of α-FeO(OH) and β-FeO(OH) [6].

The magnetization data [6] obtained on the dried biomass present a linear $M(H)$ dependence characteristic of paramagnets or magnetic particles in a superparamagnetic state. In the temperature range 100–300 K, the inverse magnetic susceptibility χ^{-1} displays linear temperature behavior. The extrapolated value of Curie temperature $\Theta = -600$ K evidences in the studied nanoparticles the exchange interaction of antiferromagnetic type. The Mössbauer spectra of dried cultures show a superposition of several quadrupole doublets due to non-equivalent states of the Fe ions in the nanoparticulate material [6].

2. EXPERIMENTAL RESULTS

As a result of the growth parameters variation of the micro-organisms (growth period, light exposure degree, potassium citrate — ferric citrate rate, etc.), different types of nanoparticles are obtained. Sample A has been separated from a bacterial biomass grown during 8 days. Sample B has been separated from a bacterial biomass grown during 21 days. From Mössbauer spectroscopy data it results that sample A is composed from ferrihydrite (chemical identical) particles.

In this study the morphology and structure of these two samples (A and B) containing biogenic iron oxide produced by *Klebsiella oxytoca* are investigated by means of a number of procedures at different length scales: optical microscopy with magnification $\times 10^2$ (Fig. 2); scanning electron microscopy with equivalent magnification $\times 4 \cdot 10^4$ (Fig. 3); and small-angle X-ray scattering with resolution $\times 10^8$ (Figs. 4 and 5).
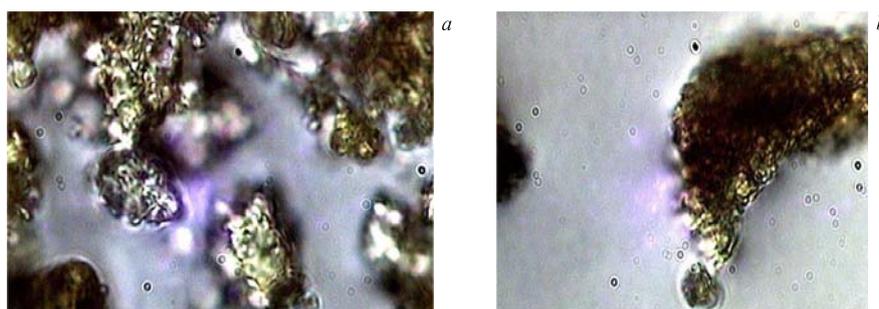
Fig. 2. Optical micrograph of sample A (*a*) and sample B (*b*)
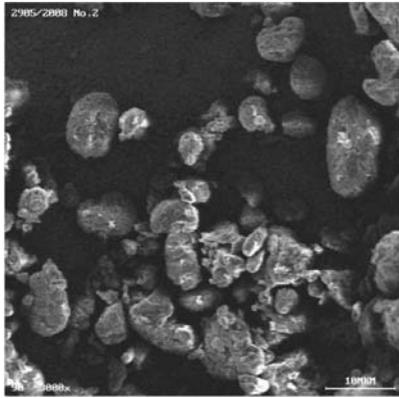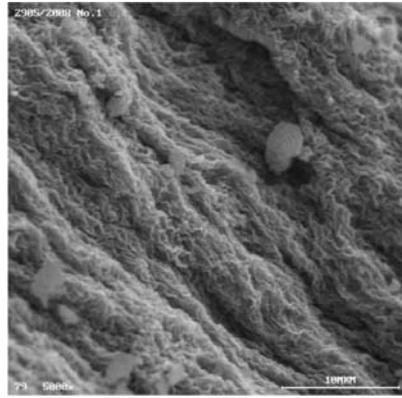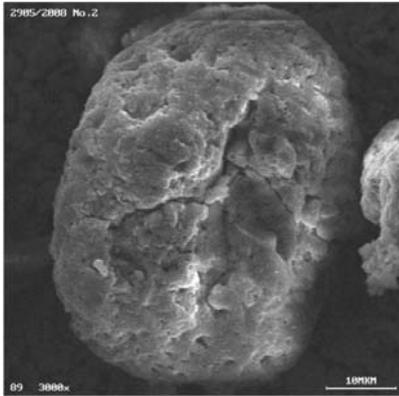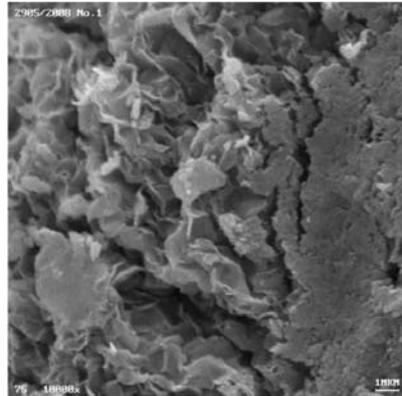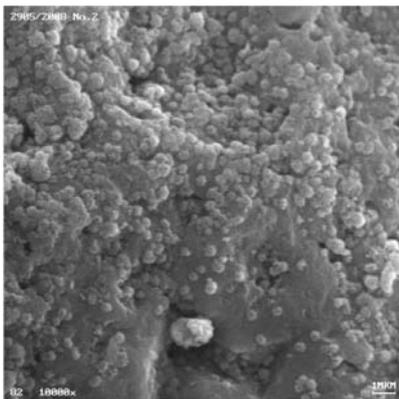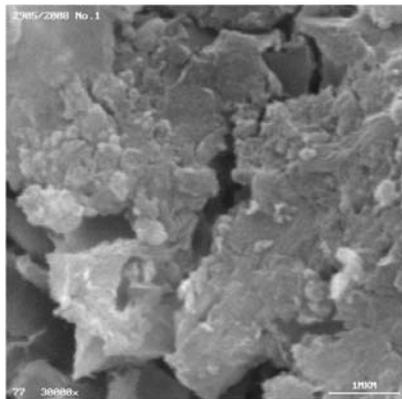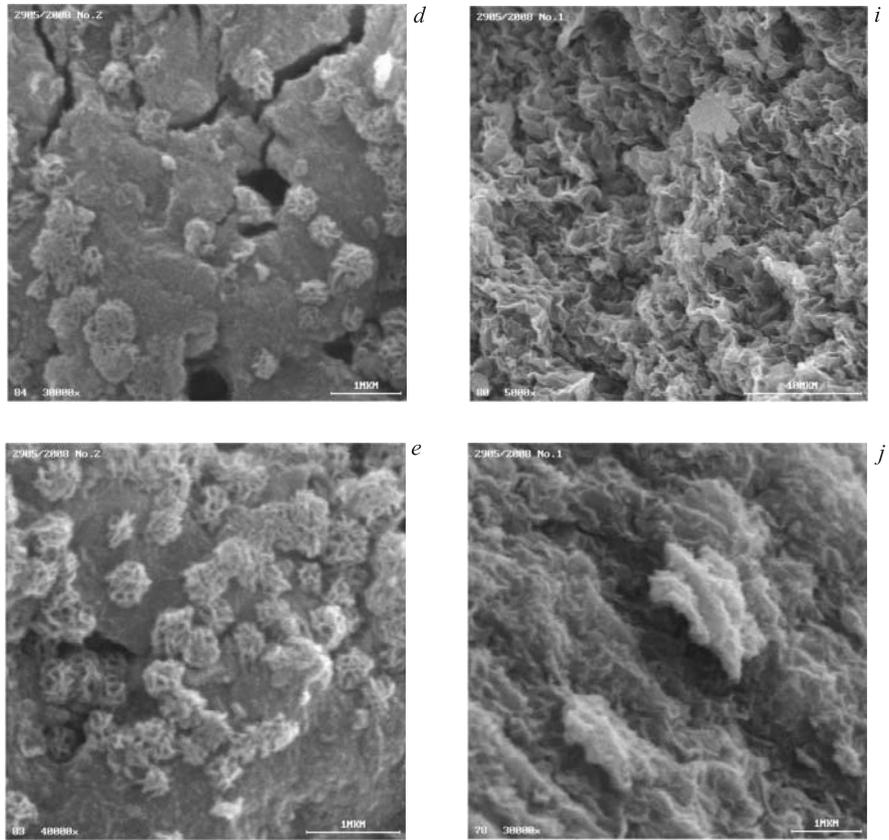
Fig. 3. SEM images of two samples containing iron oxide nanoparticles obtained by means of two different methods; sample A (a–e) and sample B (f–j)

Under the optical microscope (Microscope type Leica DM IRB), sample A looks as a polycrystalline object (Fig. 2, a), while sample B looks sponge-like (Fig. 2, b).

The images in Fig. 3 present the same samples under the JEOL type JSM-840 scanning electron microscope (SEM).

The SEM images reveal structural differences between the samples. Sample A has grain texture (Fig. 3, a); in Fig. 3, b the enlarged image of one grain is given. With a higher instrument resolution, in Fig. 3, c small entities on the grain surface are distinguished. Upon further enhancement of resolution, these entities appear as multilateral particles or clusters of smaller objects. Sample B has a stratified and friable branched texture, see Fig. 3, f–j.

5
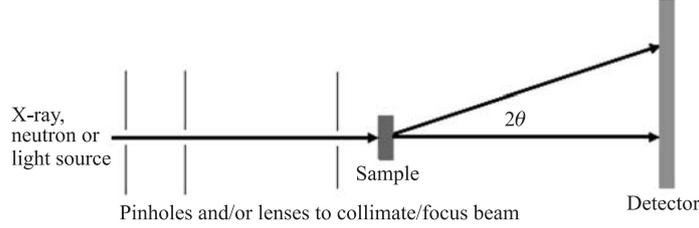
Fig. 4. Representation scheme of the small-angle scattering setup

The samples were also studied by small-angle X-ray (SAXS) method on Brucker Nanostar instrument available at the Institute of Synthetic Polymer Materials RAS, Moscow. The experimental setup used covers the q range of 0.01–0.11 Å^{-1}, see Fig. 4.

The experimental curves obtained from samples A and B reveal in the q ranges of 0.01–0.11 Å^{-1} and 0.08–0.11 Å^{-1} a power-law behavior $I(q) \approx q^{-\alpha}$, with the exponent $\alpha = 2.89 \pm 0.01$ and $\alpha = 3.18 \pm 0.01$, respectively. This means that the system has a fractal structure. When $3 < \alpha < 4$, the scattered objects are considered to be surface fractals, the fractal dimension is given by formula $D_s = 6 - \alpha$ [23]. In the case $2 < \alpha < 3$, the scattered objects are identified as mass fractals with a fractal dimension $D_m = \alpha$.

For the scattering intensity curve of sample A in the q range 0.08–0.11 Å^{-1} a mass fractal structure with the mass fractal dimension $D_m = 2.89 \pm 0.01$ is obtained. For sample B, the system structure is characterized by a fractal dimension of $D_s = 2.82 \pm 0.01$ that is specific to highly branched surface fractals. These conclusions agree with the evidence from SEM images. The maximum observed on the experimental curve of sample A at $q \approx 0.06$ Å^{-1} (Fig. 5) points out the presence of nanoparticles with the size about 100 Å that follows from relation [24]: $D = 2\pi/q$, where D is the mean dimension of the inhomogeneity producing the scattering. If the Guinier's law applies, the scattering cross section is given by the relation:

$$d\Sigma(Q)/d\Omega = d\Sigma(0)/d\Omega \exp\left(-R_g^2 q^2/3\right), \qquad (1)$$

where, $d\Sigma(0)/d\Omega$ is the scattering at zero angle and R_g is the radius of gyration of the particle, i.e., the root-mean-square distance of all scattering elements from the center of gravity. If this approximation holds, the plot $\ln[I(q)]$ vs q^2 should be linear in the small q range. With this approximation, the characteristic size of a particulate system is obtained easily. For instance, for spherical particles, one can relate the radius of particle R to the radius of gyration by $R = (5/3)^{1/2} R_g$ [25]. By applying to sample A the Guinier's law in the q range of 0.028–0.037 Å^{-1}, one gets radius of gyration as 20.42 ± 0.01 Å.

6
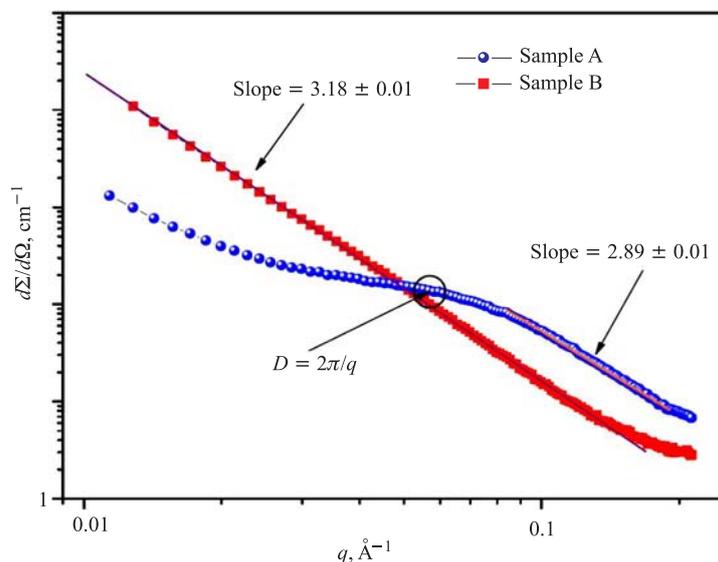
Fig. 5. SAXS experimental curves from samples A and B obtained at Brucker Nanostar SAXS spectrometer in function at the Institute of Synthetic Polymer Materials RAS, Moscow

For further investigations, complete information about composition of the samples is required. We propose SAXS and SANS studies of structural properties of the bacterial ferrihydrite samples in function of the growth conditions and the duration of the preparation processes. Comparison of polarized SANS results obtained on typical antiferromagnetic particles as Cr_2O_3, NiO and α-Fe_2O_3 with those obtained on bacterial ferrihydrite samples would be very informative for magnetic microstructure investigations [26].

REFERENCES

1. *Pankhurst Q. A., Pollard R. J.* // J. Phys.: Condens. Matter. 1993. V. 5. P. 8487–8508.

2. *Skomski R.* // J. Phys.: Condens. Matter. 2003. V. 15. P. R841–R896.

3. *Raikher Yu. L., Stepanov V. I.* // JETP. 2008. V. 134, Issue 3(9). P. 514–519 (in Russian).

4. *Sprintsova A. et al.* Nuclear Physics and Nanotechnology / Ed. A. N. Sissakian. JINR, Dubna, 2008. P. 269–277.

5. *Stolyar S. V. et al.* // Inorganic Materials. 2006. V. 42, No. 7. P. 763–768.

6. *Stolyar S. V. et al.* // Inorganic Materials. 2007. V. 43, No. 6. P. 638–641.

7. *Jambor J. L., Dutrizac J. E.* // Chem. Rev. 1998. V. 98, No. 7. P. 2549–2585.

8. *Towe K. M., Bradley W. F.* // J. Colloid Interface Sci. 1967. V. 24. P. 384.

9. *Russell J. D.* // Clay Minerals. 1979. V. 14. P. 127–138.

10. *Schwertmann U., Carlson L., Murad E.* // Clays Clay Miner. 1987. V. 35. P. 297.

11. *Huffman G. P. et al.* // Energy Fuels. 1993. V. 7. P. 285.

12. *Riveros P. A., Dutrizac J. E., Spencer P.* // Can. Metall. Q. 2001. V. 40. P. 395.

13. *Lewin A., Moore G. R., Le Brun N. E.* // Dalton Trans. 2005. V. 2005. P. 3597.

14. *Allen P. D. et al.* // Biochim. Biophys. Acta. 2000. V. 1500. P. 186.

15. *Gossuin Y. et al.* // Magnetic Resonance in Medicine. 2002. V. 48. P. 959.

16. *Kidane T. Z., Sauble E., Linder M. C.* // Am. J. Physiol.: Cell Physiol. 2006. V. 291. P. C445.

17. *Chuckrov F. V. et al.* // Intern. Geol. Rev. 1973. V. 16. P. 1131–1143.

18. *Fleischer M., Chao G. Y., Kato A.* // Am. Mineral. 1975. V. 60. P. 485–489.

19. *Janney D. E., Cowley J. M., Buseck P. R.* // Clays Clay Miner. 2000. V. 48, No. 1. P. 111–119.

20. *Janney D. E., Cowley J.M., Buseck P.R.* // Am. Mineral. 2000. V. 85. P. 1180–1187.

21. *Janney D. E., Cowley J. M., Buseck P. R.* // Am. Mineral. 2001. V. 86. P. 327–335.

22. *Stanjek H., Weidler P. G.* // Clay Minerals. 1992. V. 27. P. 397–412.

23. *Bale H.D., Schmidt P. W.* // Phys. Rev. Lett. 1984. V. 53, No. 6. P. 596–599.

24. *Klokkenburg M. et al.* // Phys. Rev. E. 2007. V. 75. P. 051408(9).

25. *Feigin L. A., Svergun D. I.* Structure Analysis by Small-Angle X-Ray and Neutron Scattering. N. Y.: Plenum Press, 1987.

26. *Yusuf S. M. et al.* // Phys. Rev. B. 2008. V. 74. P. 224428(11).

Редактор *В. В. Булатова*